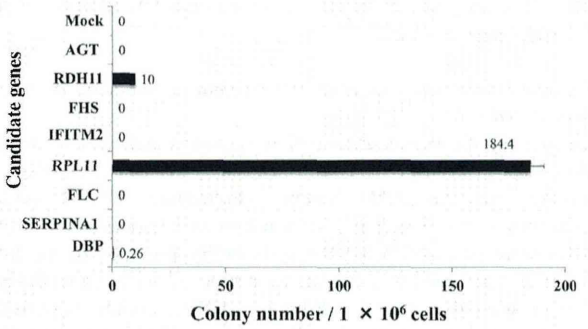

Figure 1. Identification of eight candidate genes involved in erythroid proliferation. From our screening, eight candidate genes with full-length insertions were detected. They were angiotensinogen (*AGT*), retinol dehydrogenase 11 (*RDH11*), ferritin heavy chain subunit (*FHS*), interferon-induced transmembrane protein 2 (*IFITM2*), ribosomal protein L11 (*RPL11*), ferritin light chain (*FLC*), serpin peptidase inhibitor clade A (*SERPINA1*), and D-site binding protein (*DBP*). In colony formation assays, RPL11-transduced cells yielded the highest average number of colonies (about 184). All colonies were cultured for 1 month in semisolid medium without Epo.

Results

Determination of candidate genes, and mechanisms involving in erythroid proliferation of RPL11- and RDH11-transduced cells

To identify candidate genes involved in human erythropoiesis, we first prepared lentiviruses expressing eight candidate genes, and used these viruses to transduce UT-7/Epo cells. These genes encoded angiotensinogen (AGT), ferritin heavy chain subunit (FHS), interferon-induced transmembrane protein 2 (IFITM2), ferritin light chain (FLC), ribosomal protein L11 (RPL11), retinol dehydrogenase 11 (RDH11), serpin peptidase inhibitor clade A (SERPINA1), and D-site (DBP) binding protein. After culture in semisolid medium without Epo for 1 month, we found that two of these candidate factors, RPL11 and RDH11, resulted in formation of a larger number of colonies than the other genes (RPL11, 184.4 ± 6.2; RDH11, 10.0 ± 0; Fig. 1). Colonies were positive for Venus expression (data not shown).

To further investigate cell proliferation, we next transferred the colonies derived from UT-7/Epo and RPL11- and RDH11-transduced cells into liquid culture and subjected them to proliferation assays at various time points. In the assay we used, higher absorbance at 450 nm reflected higher cell proliferation. UT-7/Epo cells incubated with Epo (■) proliferated most rapidly, whereas no proliferating cells could be detected in UT-7/Epo cells incubated without Epo (×), particularly on days 4 and 6 (Fig. 2A). In contrast to nontransduced cells, both of the RPL11- (▲) and RDH11- (●) transduced cells cultured in the absence of Epo increased cell proliferation. Compared to RDH11- (●) transduced cells, RPL11- (▲) transduced cells proliferated 2.35-, 2.67-, and 6.64-fold faster on days 2, 4, and 6, respectively; these differences were statistically significant. In addition, on day 6, RPL11- (▲) transduced cells exceeded the proliferation of UT-7/Epo cells (■) cultured in the presence of Epo. Even under the Epo-free condition, both RPL11- and RDH11-transduced cells maintained their proliferation, suggesting that the products of the transduced genes could substitute for Epo signaling in UT-7/Epo erythroleukemic cells.

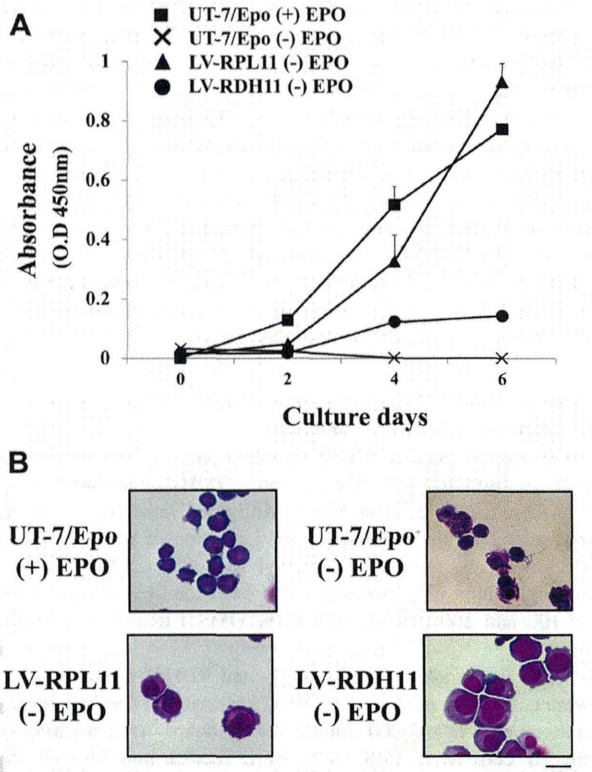

Figure 2. (**A**) Erythroid proliferation of transduced cells cultured without Epo. Cell proliferation assay of UT-7/Epo and RPL11- and RDH11-transduced cells in liquid culture. Without Epo, UT-7/Epo cells could not proliferate, whereas in the presence of Epo, these cells could proliferate very well, especially at days 2 and 4, with average ODs of 0.12 and 0.51, respectively. At day 6, RPL11-transduced cells without Epo yielded the highest cell number among these three groups, with an average OD of 0.93. (**B**) Cell morphology. UT-7/Epo cells in the presence of Epo (Upper left). UT-7/Epo cells, RPL11- and RDH11-transduced cells by lentiviruses (LV-RPL11, LV-RDH11), were cultured in the absence of Epo for 72 hours (upper right, lower left, and lower right, respectively). Cells were cytospun and subjected to May–Grunwald Giemsa staining. Scale bar = 10 um.

Morphological observation by May–Grunwald Giemsa staining indicated that by 72 hours, UT-7/Epo cells cultured without Epo had condensed nuclei and exhibited apoptotic features (Fig. 2B). On the other hand, relatively larger cells with less condensed nuclei were observed in both RPL11- and RDH11-transduced samples, compared with nontransduced cells, irrespective of the presence of Epo. This

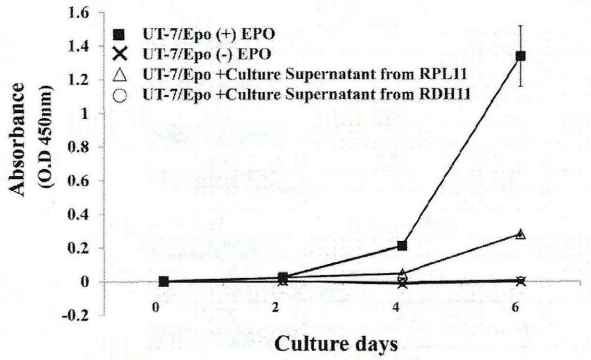

Figure 3. The proliferation of UT-7/Epo cells in the supernatant of RPL11- and RDH11-transduced cells. In order to investigate whether RPL11- and RDH11-transduced cells proliferated in an autocrine manner, UT-7/Epo cells were cultured in the absence of Epo with the supernatant of RPL11- and RDH11-transduced cells. The proliferation of UT-7/Epo cells cultured in the supernatant of RPL11- and RDH11-transduced cells was significantly decreased.

observation implies that RPL11- and RDH11-transduced cells proliferated in an immature state.

To investigate whether RPL11- and RDH11-transduced cells proliferated in autocrine manner, culture medium from respective transduced cells was used to culture UT-7/Epo without Epo. At days 4 and 6, the proliferation of UT-7/Epo cells was moderately suppressed by the culture medium from RPL11-transduced cells but completely suppressed by that from RDH11-transduced cells (Fig. 3). The Epo levels of culture supernatant of respective transduced cells were measured and were not detected, as observed with nontransduced UT-7/Epo without Epo (data not shown).

To evaluate differentiation stage, we used intracellular staining to assess Hb expression in transduced UT-7/Epo cells after 2 days of culture. Based on flow-cytometric analysis, 94.0% of UT-7/Epo cells cultured with Epo expressed β-globin, whereas only 1.2% of them expressed γ-globin. Similarly, UT-7/Epo cells cultured without Epo predominantly expressed β-globin. By contrast, both RPL11- and RDH11-transduced cells cultured without Epo expressed γ-globin (41.5% and 38.3% of cells, respectively), whereas ~30% of both types of transduced cells expressed β-globin (Supplementary Figure 1, online only, available at www.exphem.org). Taken together, these data indicate that transduction of RPL11 and RDH11 into UT-7/Epo cells induced and maintained their proliferation in an immature state.

Change of cell-cycle status in RPL11- and RDH11-transduced cells.

To investigate the mechanisms underlying proliferation, we performed cell-cycle analyses by BrdU and 7-AAD staining, followed by flow cytometry (Supplementary Figure 2, online only, available at www.exphem.org). UT-7/Epo cells cultured with Epo exhibited a prolonged S phase after 24, 48, and 72 hours of culture. On the other hand, UT-7/Epo cells cultured without Epo exhibited a reduction in the number of S-phase cells (35.0%, 17.7%, 8.2%), in accordance with increasing the number of apoptotic cells (0.5%, 5.9%, 14.8%). By contrast, both RPL11- and RDH11-transduced cells cultured without Epo exhibited a lower percentage of apoptotic cells at every time point than non-transduced cells did. UT-7/Epo cells cultured with Epo had the lowest percentage of apoptotic cells among these cell lines, whereas UT-7/Epo cultured without Epo had the highest percentage of apoptotic cells and G_2/M arrest, especially after 72 hours of culture (Fig. 4).

To clarify the mechanisms of inhibition of apoptosis in RPL11- and RDH11-transduced cells cultured without Epo, we evaluated the expression of two antiapoptotic proteins, BCL-XL and BCL-2. We found that both types of transduced cells expressed these proteins. By contrast, UT-7/Epo cultured without Epo did not express either anti-apoptotic protein, reflecting the higher percentage of apoptotic cells in this group. As previously reported [6], prominent BCL-XL expression and slight BCL-2 expression were detected in UT-7/Epo cells cultured in the presence of Epo (Fig. 5). Quantitative RT-PCR to detect BCL-XL expression also showed the same results (Fig. 6).

Signaling pathways of two transduced cell lines

To elucidate the signal transduction pathways involved in RPL11- and RDH11-driven proliferation, we performed phosphokinase array analysis after 12 hours of culture in the absence of Epo (Fig. 7A). The phosphorylation statuses of p53 (S392), Akt (T308), and AMPKa1 were almost the same among the four samples tested: UT-7/Epo cells cultured with or without Epo and RPL11- and RDH11-transduced cells cultured without Epo. The phosphorylation of p38 was the highest in UT-7/Epo cells cultured with Epo, and phosphorylation of p53 (S46) was the highest in RDH11-transduced cells. On the other hand, phosphorylation levels of both CREB and Lyn were higher in RPL11- and RDH11-transduced cells, and phosphorylated Chk-2 and AMPKa2 were upregulated in the Epo-free condition, regardless of gene transduction. Phosphorylated STAT5a (Y699) and HSP27 were downregulated in UT-7/Epo cells cultured without Epo relative to UT-7/Epo cells cultured with Epo; these phosphoproteins were upregulated in RPL11- and RDH11-transduced cells to the same level as in UT-7/Epo with Epo (Fig. 7B).

To ascertain that STAT5 signaling pathway was involved in the proliferation of RPL11- and RDH11-transduced cells, we conducted phosphokinase array and proliferation assay using these cells in the presence of STAT5 inhibitor. Our results from phosphokinase array confirmed that STAT5 phosphorylation was dramatically decreased in the presence of STAT5 inhibitor (Fig. 8A). Importantly, proliferation assay revealed that RDH11-transduced cells showed significantly decreased proliferation at any observed points in the presence of 100 and

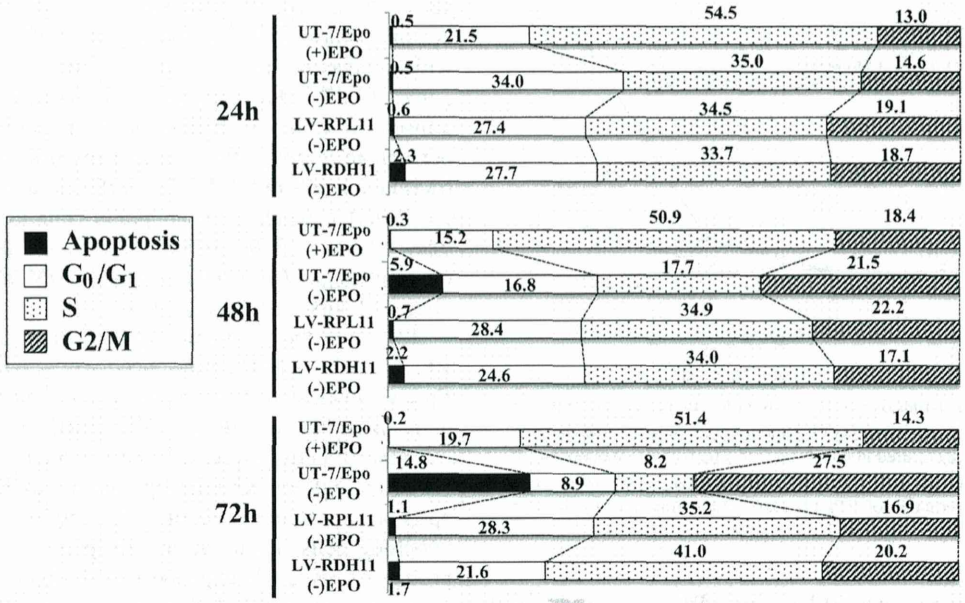

Figure 4. Cell-cycle determination of three cell lines. At 24, 48, and 72 hours after cultured, cells were collected and analyzed with flow cytometry. UT-7/Epo cells without Epo exhibited the highest apoptosis and G_2/M arrest at 72 hours (14.8% and 27.5% of cells, respectively). The lowest percentage of apoptosis and the highest percentage of S phase arrest at every time point were observed in UT-7/Epo cultured with Epo. Between the 2 types of transduced cells, RPL11-transduced cells exhibited the lower percentage of apoptosis than RDH11-transduced cells, especially at 24 and 48 hours. Q35

200 μmol/L STAT5 inhibitor, whereas RPL11-transduced cells showed significantly decreased proliferation only at day 2 in the presence of 200 μmol/L STAT5 inhibitor (Fig. 8B). CREB, Lyn, and JAK2 phosphorylation were also studied using immunocytochemistry, and the phosphorylation of both CREB and Lyn were observed (Fig. 8C). Of note, the phosphorylation of JAK2 could not be demonstrated in our study (data not shown).

To further examine STAT-5 regulated genes, we observed the expression of *PIM2* and *CCND1* by real-time PCR analysis [7,8]. The results showed that *PIM2* expressions were not different among the samples, but *CCND1* expression was elevated by 43.4-fold in RDH11-transduced cells and 2.5-fold in RPL11-transduced cells compared with those in the UT-7/Epo control (Fig. 9).

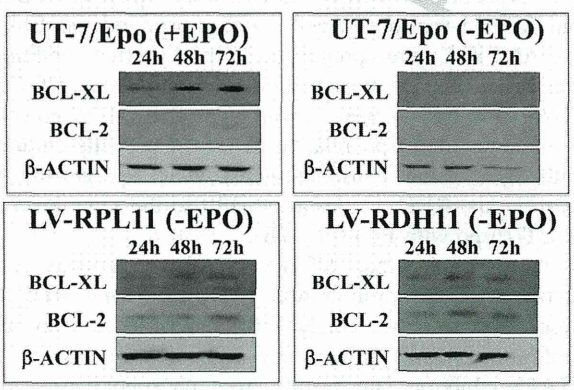

Figure 5. Expression of antiapoptotic proteins was demonstrated by Western blotting. Neither BCL-XL nor BCL-2 was detected in UT-7/Epo cultured without Epo, whereas the expression level of BCL-XL was higher than that of BCL-2 in UT-7/Epo cultured with Epo. Both types of transduced cells also expressed BCL-XL and BCL-2 at every time point. β-ACTIN was used as internal control.

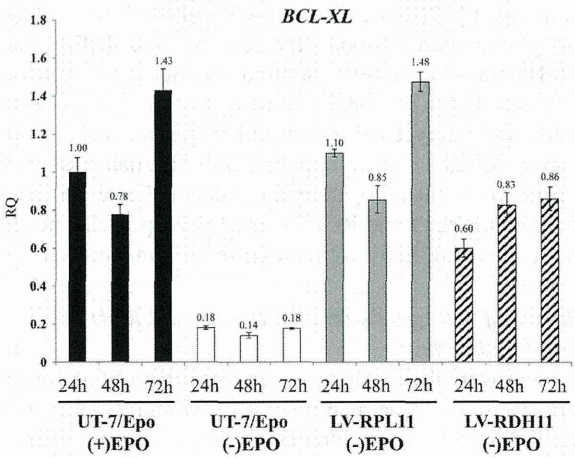

Figure 6. Quantitative RT-PCR of *Bcl-xL* gene. The expression of *Bcl-xL* gene of RPL11- and RDH11-transduced cells was demonstrated. The highest expression was detected in all cell lines at 72 hours. *RQ* = ■■■. Q36

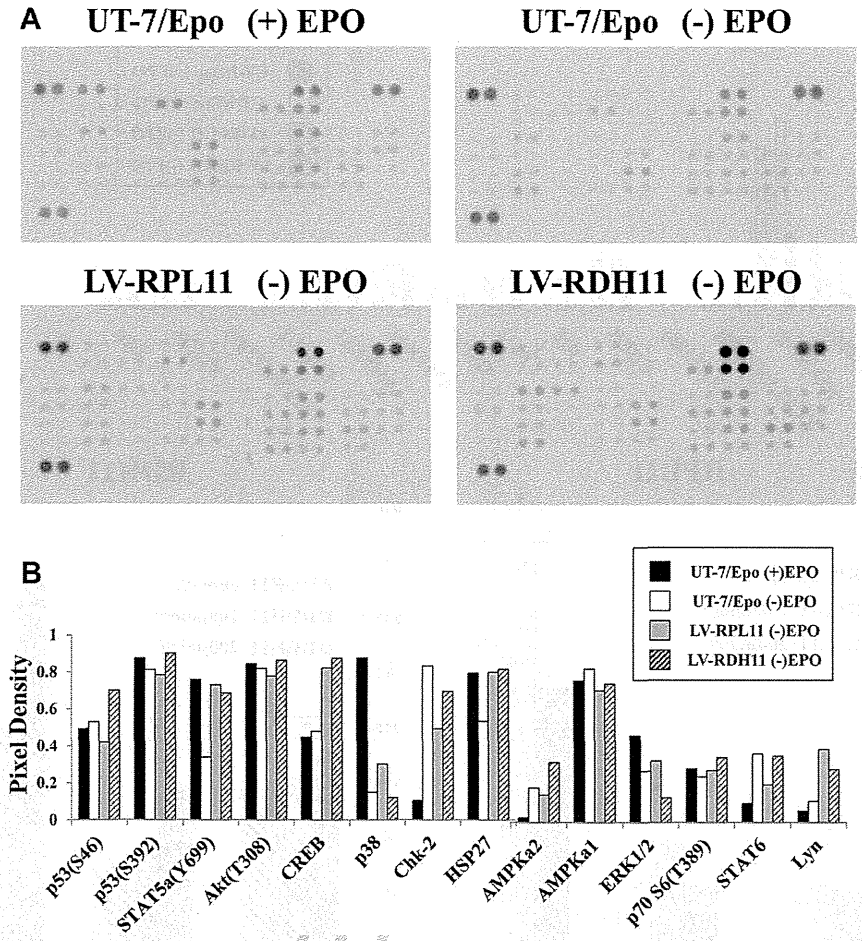

Figure 7. (**A**) Pixel densities of phosphokinase arrays performed on three cell lines. After 12 hours, cells were lysed with lysis buffer and further processed for detection of kinase activation. Pixel densities were evaluated and analyzed using LAS3000 (Fuji Film Co., Tokyo, Japan). (**B**) Determination of signaling pathways in UT-7/Epo and both types of transduced cells. Phosphokinase arrays performed on three cell lines demonstrated that STAT5a (Y699) activation was markedly reduced in UT-7/Epo cultured without Epo, with a pixel density of ~0.4. In UT-7/Epo cultured with Epo, the level of STAT5a (Y699) phosphorylation was almost at the same as in both types of transduced cells cultured with Epo, with a pixel density of ~0.8. The Akt (T308) and AMPKa1 pathways were also activated at almost the same level in all cell lines, with pixel densities of ~0.8. CREB, and Lyn kinases were predominantly activated only in transduced cells, with pixel density ratios (transduced cells vs. UT-7/Epo cells) of ~2.

Discussion

Our findings indicate that the overexpression of RPL11 and RDH11 can maintain the growth and proliferation of UT-7/Epo cells in culture conditions in the absence of Epo. Interestingly, the proliferation of both of RPL11- and RDH11-transduced cells was not due to autocrine manner as shown in Figure 3. Gene transfer of *RPL11* to UT-7/Epo cells resulted in more increased number of cells and colonies than that of *RDH11*. In addition, the percentage of apoptotic cells in RPL11-transduced cells was much lower than that in RDH11-transduced cells. Therefore, it is possible that RPL11 has greater potential than RDH11 to induce the proliferation of UT-7/Epo cells. RPL11 has been recently demonstrated to be essential for normal cell proliferation by supporting ribosomal biogenesis and transcription capacity [9]. In the special context of erythroid proliferation, RPL11 has been previously reported to increase the translation of a specific set of transcripts, such as Bag1, which encodes an Hsp70 cochaperone, and Csde1, which encodes an RNA-binding protein, and both were expressed at increased levels in erythroblasts [10]. A recent report using zebrafish embryos also showed that RPL11 could support hematopoietic iron metabolism and Hb synthesis, whereas the promotion of erythroid proliferation by RDH11 is due to all-*trans*-retinoic acid, an active metabolite of this enzyme's catalytic process [11–13]. As demonstrated in this study, these effects result in promotion of erythroid proliferation by RPL11 and RDH11. Notably, increased expression level of *RDH11* gene in UT-7/Epo cells might not significantly increase the level of retinoic acids produced in these cells, because the substrate for the enzymatic reaction is limited. Moreover, the apoptosis

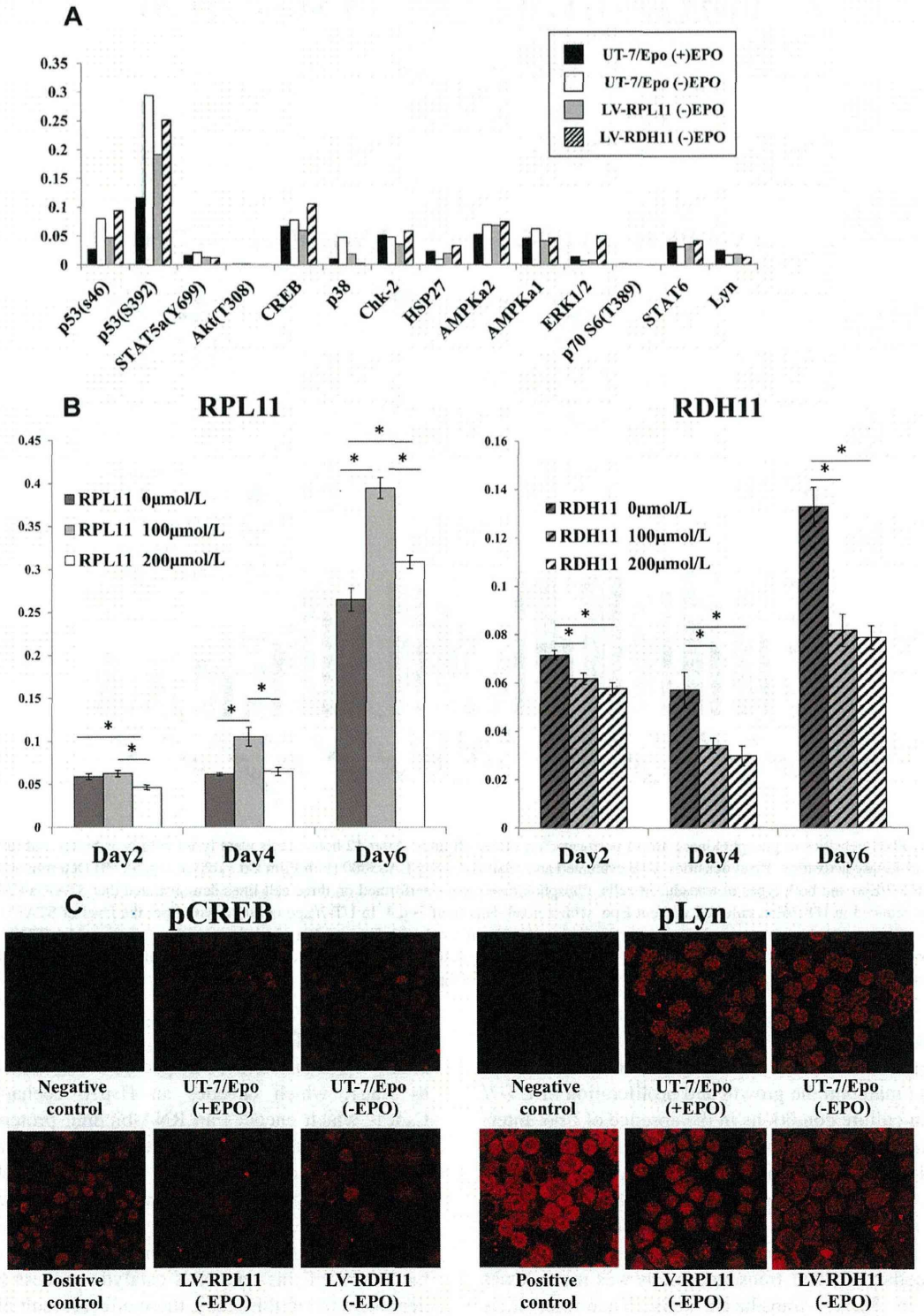

web 4C/FPO

Figure 8. (**A**) Phospho-kinase array with STAT5 inhibitor at a final concentration of 100 μmol/L for 12 hours. To ascertain the STAT5 signaling pathway involved in RPL11- and RDH11-transduced cells, STAT5 inhibitor was added in the culture medium. STAT5a (Y699) was demonstrated to be significantly decreased by phosphokinase array. (**B**) Cell proliferation assays of RPL11- and RDH11-transduced cells with STAT5 inhibitor. RPL11- and RDH11-transduced cells were cultured for 2, 4, and 6 days in the presence of STAT5 inhibitor at final concentrations of 100 and 200 μmol/L. Cells were harvested and processed for proliferation assay. At day 2, the proliferations of RPL11- and RDH11-transduced cells were significantly inhibited at 200 μmol/L of STAT5 inhibitor. * . (**C**) The phosphorylation of CREB and Lyn using immunocytochemistry. UT-7/Epo with or without Epo, and RPL11- and RDH11-transduced cells were harvested and processed for immunocytochemistry. The phosphorylation of CREB and Lyn was demonstrated. Q37

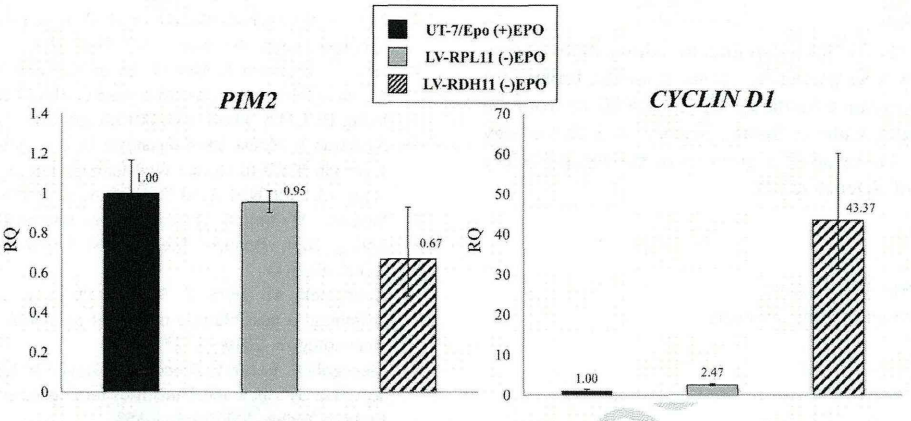

Figure 9. Quantitative RT-PCR of STAT5 target genes. The expression of *PIM2* did not differ significantly among the samples (left). By contrast, *CCND1* was upregulated in RPL11-and RDH11-transduced cells (2.47- and 43.37-fold, respectively) relative to the control UT-7/Epo cells (right). *RQ* = ■■■.

induced by retinoic acid might be another reason that RDH11-transduced cells proliferate less rapidly than those transduced with RPL11 [14]. Only 30% of RPL11- and RDH11-transduced cells could produce â-globin, compared with 80% of UT-7/Epo cells. Several possibilities might explain this reverse switching, including increased expression of specific miRNAs [15–18]. In RDH11-transduced cells, retinoic acid can also inhibit HDACs, resulting in activation of transcriptional processes and ultimately increased expression of γ-globin [19].

Our experiments also demonstrated that STAT5a was markedly activated to almost the same extent in all cell lines, whereas the CREB and Lyn kinases were highly activated in RPL11-and RDH11-transduced cells. Lyn is a hematopoiesis-specific kinase, and its role in erythroid precursors has also been identified. Lyn activation triggers phosphorylation of STAT5 molecules by phosphorylation of protein phosphatase SHP-1 [20,21]. Activation of CREB by the cAMP signaling pathway can also induce STAT5 activation [22,23]. By inhibition of STAT5 activity using STAT5 inhibitor, the proliferation of both RPL11- and RDH11-transduced cells significantly decreased, especially at day 2 with the dosage of 200 μmol/L (Fig. 8B). Thus, it appears that activation of STAT5 was specifically involved in erythroid proliferation in both types of transduced cells, in accordance with a previous report [24]. Surprisingly, our data showed that STAT5 inhibitor could inhibit the proliferation of RPL11-transduced cells, but not as strongly as that of RDH11-transduced cells. This observation indicates that the signaling pathways involving in proliferation of RPL11-transduced cells might be more complex. Moreover, the JAK2 phosphorylation could not be demonstrated in our study. From previous report, JAK2 phosphorylation could be detected for only a 2-hour interval immediately after adding Epo into the Epo-deprived culture medium [25]. Another important possibility is that JAK2 activation is not the upstream signaling pathway of STAT5 in our conditions. Thus, STAT5 phosphorylation in both RPL11- and RDH11-transduced cells may be the direct activation resulting from Lyn and CREB phosphorylation.

The activation of antiapoptotic proteins, BCL-XL and BCL-2, by STAT5 might also be one of the mechanisms that maintains the growth and survival of these cells [26]. Furthermore, *CCND1* expression was highly upregulated in both types of transduced cells, especially in RDH11-transduced cells. STAT5 can induce *CCND1* expression, thereby stimulating cell-cycle progression and further inducing proliferation [27–29]. However, the high accumulation of *CCND1* at day 3 in RDH11-transduced cells might have been due to their active entries from G_0/G_1 to late S phases, concomitant with the accumulation at G_2/M phases, as demonstrated in RDH11 cell cycle determination at 72 hours [27].

In conclusion, our study demonstrates that both of RPL11 and RDH11 can induce proliferation in the UT-7/Epo cell line in the absence of Epo. Our data provide more insights into the mechanisms underlying induction of erythroid proliferation, a promising treatment strategy for patients with conditions such as Diamond–Blackfan anemia (DBA). DBA is caused by mutations of components of the small and large ribosomal subunits, such as RPL5 and RPL11 [30–32]. Therefore, transduction of RPL11 should help to improve patients' symptoms and signs. In addition, transduction of RDH11 results in increased synthesis of all-*trans*-retinoic acid, a potential therapeutic approach for treating the refractory anemia in myelodysplastic syndromes [33]. Our findings also indicate that STAT5 activation is involved in this proliferation process. Finally, CREB and Lyn protein kinases might participate in the activation of STAT5 in our transduced cells, resulting in further upregulation of *CCND1* expression.

Acknowledgement

We are thankful to Ms. Michiko Ushijima for administrative assistance. This work was supported by grants from the Project for Realization of Regenerative Medicine (K.T., 08008010) from the Ministry of Education, Culture, Sports, Science, and Technology (MEXT) of Japan. TK received a grant from the Japan Society for the Promotion of Science (JSPS).

Conflict of interest disclosure

The authors have no competing interests.

References

1. Komatsu N, Yamamoto M, Fujita H, et al. Establishment and characterization of an erythropoietin-dependent subline, UT-7/Epo, derived from human leukemia cell line, UT-7. Blood. 1993;82:456–464.
2. Inoue T, Sugiyama D, Kurita R, et al. APOA-1 is a novel marker of erythroid cell maturation from hematopoietic stem cells in mice and humans. Stem Cell Rev. 2011;7:43–52.
3. Kurita R, Oikawa T, Okada M, et al. Construction of a high-performance human fetal liver-derived lentiviral cDNA library. Mol Cell Biochem. 2008;319:181–187.
4. Stegeman H, Kaanders J, Verheijen M, et al. Combining radiotherapy with MEK1/2, STAT5 or STAT6 inhibition reduces survival of head and neck cancer cells. Mol Cancer. 2013;12:133.
5. Hamadi A, Deramaudt T, Takeda K, Ronde P. Hyperphosphorylated FAK delocalizes from focal adhesions to membrane ruffles. J Oncol. 2010;2010:932803.
6. Uchida M, Kirito K, Endo H, Ozawa K, Komatsu N. Activation of FKHRL1 plays an important role in protecting erythroid cells from erythropoietin deprivation – induced apoptosis in a human erythropoietin-dependent leukemia cell line, UT-7/EPO. Int J Hematol. 2007;86:315–324.
7. Basham B, Sathe M, Grein J, et al. In vivo identification of novel STAT5 target genes. Nucleic Acids Res. 2008;36:3802–3818.
8. Matsumura I, Kitamura T, Wakao H, et al. Transcriptional regulation of the cyclin D1 promoter by STAT5: its involvement in cytokine-dependent growth of hematopoietic cells. EMBO J. 1999;18:1367–1377.
9. Teng T, Mercer CA, Hexley P, et al. Loss of tumor suppressor RPL5/RPL11 does not induce cell cycle arrest but impedes proliferation due to reduced ribosome content and translation capacity. Mol Cell Biol. 2013;33:4660–4671.
10. Horos R, Jspeert H, Pospisilova D, et al. Ribosomal deficiencies in Diamond-Blackfan anemia impair translation of transcripts essential for differentiation of murine and human erythroblasts. Blood. 2012;119:262–272.
11. Zhang Z, Jia H, Zhang Q, et al. Assessment of hematopoietic failure due to Rpl11 deficiency in a zebrafish model of Diamond-Blackfan anemia by deep sequencing. BMC Genomics. 2013;14:896.
12. Liden M, Eriksson U. Understanding retinol metabolism: Structure and function of retinol dehydrogenases. J Biol Chem. 2006;281:13001–13004.
13. Douer D, Koeffler P. Retinoic acid enhances growth of human early erythroid progenitor cells in vitro. J Clin Invest. 1982;69:1039–1041.
14. Noy N. Between death and survival: Retinoic acid in regulation of apoptosis. Annu Rev Nutr. 2010;30:201–217.
15. Lulli V, Romania P, Morsilli O, et al. MicroRNA-486-3p regulates gamma-globin expression in human erythroid cells by directly modulating BCL11A. PLoS One. 2013;8:e60436.
16. Sankaran V, Menne TF, Scepanovic D, et al. MicroRNA-15a and - 16-1 act via MYB to elevate fetal hemoglobin expression in human trisomy 13. Proc Natl Acad Sci U S A. 2011;108:1519–1524.
17. Sankaran V, Orkin S. The switch from fetal to adult hemoglobin. Cold Spring Harb Perspect Med. 2013; http://dx.doi.org/10.1101/cshperspect.a011643.
18. Gabbianelli M, Testa U, Morsilli O, et al. Mechanism of human switching: a possible role of the kit receptor/miR 221-222 complex. Hematologica. 2010;95:1253–1260.
19. Menegola E, Renzo F, Broccia M, Giavini E. Inhibition of histone deacetylase as a new mechanism of teratogenesis. Birth Defects Res C Embryo Today. 2006;78:345–353.
20. Ingley E. Functions of the Lyn tyrosine kinase in health and disease. Cell Commun Signal. 2012;10:21.
21. Xiao W, Ando T, Wang HY, et al. Lyn-and PLC-β3-dependent regulation of SHP-1 phosphorylation controls STAT5 activity and myelomonocytic leukemia-like disease. Blood. 2010;116:6003–6013.
22. Delghandi MP, Johannessen M, Moens U. The cAMP signaling pathway activates CREB through PKA, p38 and MSK1 in NIH3T3 cells. Cell Signal. 2005;17:1343–1351.
23. Boer AK, Drayer AL, Vellenga E. Stem cell factor enhances erythropoietin-mediated transactivation of signal transducer and activator of transcription 5 (STAT5) via the PKA/CREB pathway. Exp Hematol. 2003;31:512–520.
24. Schepers H, Wierenga A, Vellenga E, Schuringa J. STAT5-mediated self-renewal of normal hematopoietic and leukemic stem cells. JAK-STAT. 2012;1:13–22.
25. Erickson-Miller C, Pelus L, Lord K. Signaling induced by erythropoietin and stem cell factor in UT-7/Epo cells: transient versus sustained proliferation. Stem Cell. 2000;18:366–373.
26. Koulnis M, Porpiglia E, Porpiglia P, et al. Contrasting dynamic responses in vivo of the Bcl-XL and Bim erythropoietic survival pathways. Blood. 2012;119:1228–1239.
27. Stacey DW. Cyclin D1 serves as a cell cycle regulatory switch in actively proliferating cells. Curr Opin Cell Biol. 2003;15:158–163.
28. Baldin V, Lukas J, Marcote M, Pagano M, Draetta G. Cyclin D1 is a nuclear protein required for cell cycle progression in G1. Genes Dev. 1993;7:812–821.
29. de Groot RP, Raaijmakers JA, Lammers JW, Koenderman L. STAT5-dependent cyclinD1 and Bcl-XL expression in Bcr-abl transformed cells. Mol Cell Biol Res Commun. 2000;3:299–305.
30. Moniz H, Gastou M, Leblanc T, et al. Primary hematopoietic cells from DBA patients with mutations in RPL11 and RPS19 genes exhibit distinct erythroid phenotype in vitro. Cell Death Dis. 2012;3:e356.
31. Vlachos A, Ball S, Dahl N, et al. Diagnosing and treating Diamond Blackfan anaemia: results of an international clinical consensus conference. Br J Haematol. 2008;142:859–876.
32. Robledo S, Idol R, Crimmins D, Ladenson J, Mason P, Bessler M. The role of human ribosomal proteins in the maturation of rRNA and ribosome production. RNA. 2008;14:1918–1929.
33. Itzykson R, Ayari S, Vassilief D, et al. Is there a role for all-trans retinoic acid in combination with recombinant erythropoietin in myelodysplastic syndromes? A report on 59 cases. Leukemia. 2009;23:673–678.

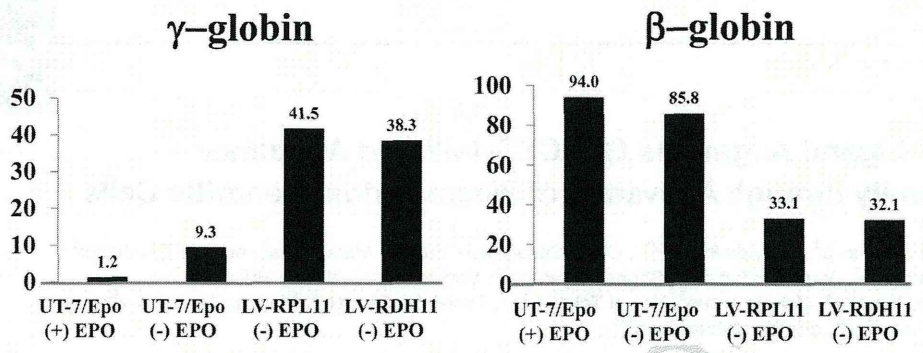

Supplementary Figure 1. Analysis of hemoglobin content in RPL11- and RDH11-transduced cells. Hemoglobin production in both types of transduced cells was compared with that in the parental UT-7/Epo cells. Switching of hemoglobin type was demonstrated to have occurred: adult hemoglobin (β-globin) was highly expressed in UT-7/Epo cells, whereas fetal hemoglobin (γ-globin) was highly expressed in both types of transduced cells.

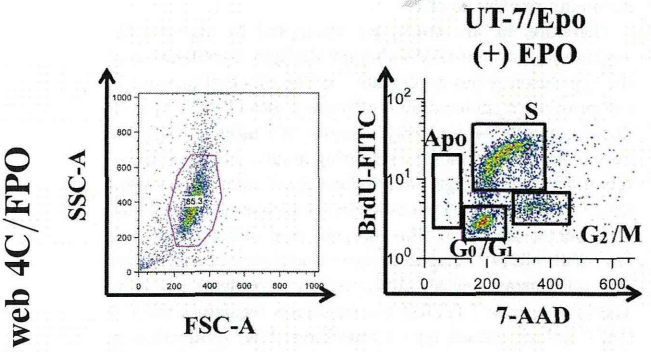

Supplementary Figure 2. Cell cycle determination using FITC-conjugated anti-BrdU, analyzed by flow cytometry of UT-7/Epo cultured with Epo. The G_0/G_1, S, G_2/mol/L, and apoptotic groups were gated as shown.

Published OnlineFirst April 10, 2014; DOI: 10.1158/2326-6066.CIR-13-0143

Research Article

Cancer Immunology Research

TLR7 Ligand Augments GM-CSF–Initiated Antitumor Immunity through Activation of Plasmacytoid Dendritic Cells

Megumi Narusawa[1], Hiroyuki Inoue[1,2,3], Chika Sakamoto[1], Yumiko Matsumura[1], Atsushi Takahashi[1], Tomoko Inoue[1], Ayumi Watanabe[1], Shohei Miyamoto[1], Yoshie Miura[1], Yasuki Hijikata[3], Yoshihiro Tanaka[3], Makoto Inoue[5], Koichi Takayama[2], Toshihiko Okazaki[4], Mamoru Hasegawa[5], Yoichi Nakanishi[2], and Kenzaburo Tani[1,3]

Abstract

Vaccination with irradiated granulocyte macrophage colony-stimulating factor (GM-CSF)–transduced autologous tumor cells (GVAX) has been shown to induce therapeutic antitumor immunity. However, its effectiveness is limited. We therefore attempted to improve the antitumor effect by identifying little-known key pathways in GM-CSF–sensitized dendritic cells (GM-DC) in tumor-draining lymph nodes (TDLN). We initially confirmed that syngeneic mice subcutaneously injected with poorly immunogenic Lewis lung carcinoma (LLC) cells transduced with Sendai virus encoding GM-CSF (LLC/SeV/GM) remarkably rejected the tumor growth. Using cDNA microarrays, we found that expression levels of type I interferon (IFN)–related genes, predominantly expressed in plasmacytoid DCs (pDC), were significantly upregulated in TDLN-derived GM-DCs and focused on pDCs. Indeed, mouse experiments demonstrated that the effective induction of GM-CSF–induced antitumor immunity observed in immunocompetent mice treated with LLC/SeV/GM cells was significantly attenuated when pDC-depleted or IFNα receptor knockout ($IFNAR^{-/-}$) mice were used. Importantly, in both LLC and CT26 colon cancer–bearing mice, the combinational use of imiquimod with autologous GVAX therapy overcame the refractoriness to GVAX monotherapy accompanied by tolerability. Mechanistically, mice treated with the combined vaccination displayed increased expression levels of CD86, CD9, and Siglec-H, which correlate with an antitumor phenotype, in pDCs, but decreased the ratio of $CD4^+CD25^+FoxP3^+$ regulatory T cells in TDLNs. Collectively, these findings indicate that the additional use of imiquimod to activate pDCs with type I IFN production, as a positive regulator of T-cell priming, could enhance the immunologic antitumor effects of GVAX therapy, shedding promising light on the understanding and treatment of GM-CSF–based cancer immunotherapy. *Cancer Immunol Res; 2(6); 568–80. ©2014 AACR.*

Introduction

In recent clinical trials of patients with diverse solid cancers, cancer immunotherapy such as therapeutic vaccination with granulocyte macrophage colony-stimulating factor (GM-CSF) gene-transduced tumor vaccines (GVAX), as well as sipuleucel-T (Provenge; Dendreon), the first FDA-approved GM-CSF–based therapeutic dendritic cell (DC) vaccine for prostate cancer, induced antitumor immune responses with tolerability (1–3). However, the efficacy of this therapy alone is not satisfactory, raising an urgent need to improve the antitumor effect of GVAX. Although GM-CSF signaling is essential in conventional DC (cDC) maturation, which leads to effective generation of tumor-associated antigen (TAA)-specific T cells and differentiation, the underlying molecular mechanism of how GM-CSF sensitizes and matures DCs (GM-DC, i.e., GM-CSF–sensitized DCs) to trigger host antitumor immunity remains unclear.

Therefore, in this study, we attempted to improve the antitumor effects of GVAX therapy through identification of the key cluster genes upregulated in GM-DCs that operate T-cell priming in tumor-draining lymph nodes (TDLN) by conducting a cDNA microarray analysis. We used a syngeneic Lewis lung carcinoma (LLC)–bearing mouse, which exhibited remarkable tumor regression following subcutaneous administration of fusion (F) gene-deleted nontransmissible Sendai virus vector–mediated GM-CSF gene-transduced LLC (LLC/SeV/GM) cells (4). Using this experimental system, the expression microarray analysis elucidated that pathways involving Toll-like receptor 7 (TLR7) and interferon regulatory factor 7 (IRF7), which induce type I interferon (IFN) production in plasmacytoid DCs (pDC; ref. 5), were upregulated in GM-CSF–activated mature DCs. Further activation of this pathway using

Authors' Affiliations: [1]Department of Molecular Genetics, Medical Institute of Bioregulation; [2]Research Institute for Diseases of the Chest, Graduate School of Medical Sciences; [3]Department of Advanced Cell and Molecular Therapy and [4]Center for Clinical and Translational Research, Kyushu University Hospital, Kyushu University, Fukuoka; and [5]DNAVEC Corporation, Tsukuba, Japan

Note: Supplementary data for this article are available at Cancer Immunology Research Online (http://cancerimmunolres.aacrjournals.org/).

Corresponding Author: Kenzaburo Tani, Department of Molecular Genetics, Medical Institute of Bioregulation, Kyushu University, 3-1-1 Maidashi, Higashi-ku, Fukuoka 812-8582, Japan. Phone: 81-92-642-6449; Fax: 81-92-642-6444; E-mail: taniken@bioreg.kyushu-u.ac.jp

doi: 10.1158/2326-6066.CIR-13-0143

Published OnlineFirst April 10, 2014; DOI: 10.1158/2326-6066.CIR-13-0143

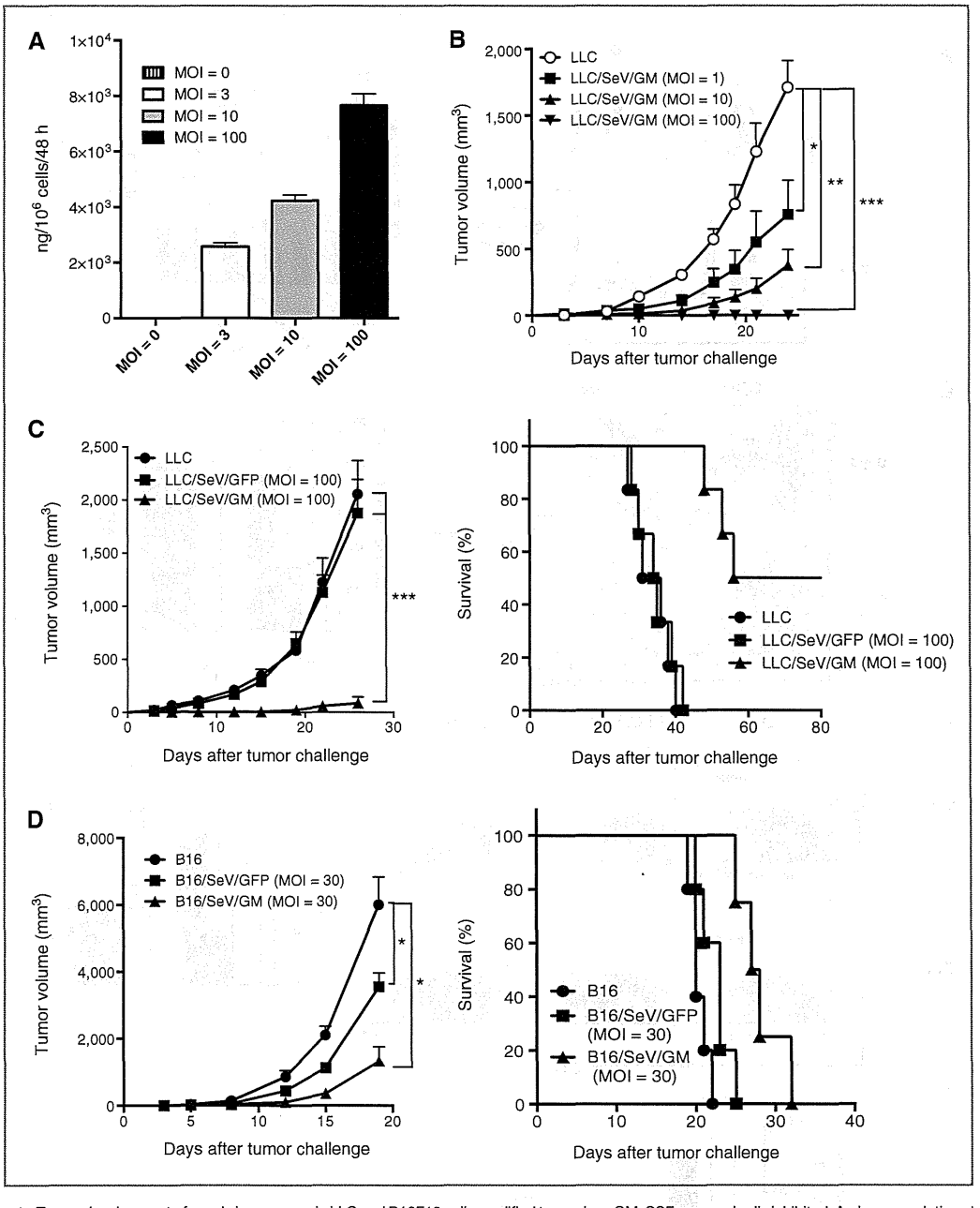

Figure 1. Tumor development of poorly immunogenic LLC and B16F10 cells modified to produce GM-CSF was markedly inhibited. A, dose-escalation studies to assess GM-CSF production from LLC/SeV/GM cells (MOI = 0, 3, 10, and 100). GM-CSF production levels in the supernatants from the 48-hour culture were measured by ELISA. B and C, tumorigenicity assays using LLC cells. B, a total of 3.0×10^5 LLC and LLC/SeV/GM (MOI of 1, 10, or 100) cells were subcutaneously inoculated into the right flank of C57/BL6N mice ($n = 3$). C, a total of 2.0×10^5 LLC, LLC/SeV/GFP, or LLC/SeV/GM (MOI = 100) cells were inoculated into the right flank of C57/BL6N mice ($n = 6$). Significant tumor regression (left) and prolonged survival (right) was shown in mice treated with LLC/SeV/GM cells. D, tumorigenicity assays using B16F10 cells. In total, 1.0×10^5 B16F10, B16/SeV/GFP, or B16/SeV/GM (MOI = 30) cells were inoculated into the right flanks of C57/BL6N mice ($n = 6$). Significant tumor regression (left) and prolonged survival (right) were observed in mice treated with B16/SeV/GM cells. The asterisks indicate statistically significant differences (*, $P < 0.05$; **, $P < 0.01$; ***, $P < 0.001$). Kaplan–Meier survival curves are shown, and mortality was determined by the log-rank test (LLC vs. LLC/SeV/GM and LLC/SeV/GFP vs. LLC/SeV/GM; $P < 0.001$, LLC vs. LLC/SeV/GFP; $P = 0.67$, B16 vs. B16/SeV/GM and B16/SeV/GFP vs. B16/SeV/GM; $P < 0.05$).